

Eliminating harmonic noise in vibroseis data through sparsity-promoted waveform modeling

Dawei Liu¹, Xiangfang Li¹, Wei Wang², Xiaokai Wang¹, Zhensheng Shi¹, and Wenchao Chen¹

ABSTRACT

Vibroseis acquisition, which uses slip sweep instead of traditional flip-flop acquisition, could significantly reduce cycle time and increase productivity. However, the vibroseis system suffers from harmonically distorted sweeps being used as correlation operators, thus causing sticky harmonic distortions in correlated data that cannot be eliminated by forerunning manipulations and hindering interpretation. We propose a novel method to separate the harmonic interferences from correlated vibroseis data by exploring the waveform diversity between useful reflections and harmonic interferences. Following the diverse time-frequency distribution patterns of useful signal components and harmonic interferences, two different redundant waveform dictionaries are constructed to sparsely model useful reflections and harmonic interferences. Then, an iterative thresholding algorithm is used to gradually separate harmonic interferences from useful reflections, with each successive iteration potentially extracting the most reliable waveform elements built up into the corresponding signal components. The processing results of synthetic and field data examples highlight the effectiveness of our method in eliminating harmonic noise without noticeable loss of useful reflections. Compared to the classic frequency-dependent attenuation method, our approach has a higher fidelity.

INTRODUCTION

Sustaining data quality and productivity improvements in the land seismic industry is necessary to fulfill the growing demand for low-cost, high-density, and wide-azimuth recordings. The vibroseis

system has been widely used in the land seismic industry, becoming the preferred seismic energy source, especially when international oil prices fluctuate and remain low. It can support highly efficient seismic production and avoid pollution caused by dynamite sources.

After crosscorrelation with the sweep, vibroseis data produced by modern equipment using high signal-to-noise recording techniques commonly deliver well-defined zero-phase wavelets. However, several anomalous signals have been shown to occur in the original data following the correlation process using this recording technique. Therefore, many methods are used for data enhancement during vibroseis recording and processing in the field, such as amplitude control, vibrator phase control, correlation, spike, and spectral noise reduction. For example, spike noise arising from uncorrelated data was challenging because it reproduces the sweep signal in a time-reversed sequence. This impact may partly or entirely distort the valuable information in the correlated data, depending on the temporal location of the spike in the uncorrelated data. This distortion is no longer an issue in vibroseis data recording when using current recording systems with real-time spike noise attenuation. But beyond this, harmonic distortion is another known noise factor that still challenges vibroseis data recording. Ideally, the vibrator is expected to generate a sweep, also known as the pilot signal, which is the reference of the fundamental component. However, because of the harmonic distortion associated with the fundamental sweep, the output signal generated by the vibrator is significantly different from the pilot signal; therefore, it is referred to as a harmonically distorted sweep. The nonlinear coupling effect between the vibrator and soil is a well-known cause of harmonic distortions (Lebedev and Beresnev, 2004). Correlated harmonics produce noise in ghosts multiple times from the primary when the recorded data are compressed by correlating with the pilot signal or reference. In addition, in up-sweep surveys, the harmonic noise is shifted to the negative time domain, whereas in down-sweep surveys, the harmonic noise is moved to the positive time domain.

Because of nonlinear effects, including the nonlinear coupling between the baseplate and the ground, the inadequacy of the feedback

Manuscript received by the Editor 10 July 2021; revised manuscript received 25 December 2021; published ahead of production 24 January 2022; published online 8 March 2022.

¹Xi'an Jiaotong University, School of Information and Communications Engineering, Xi'an 710049, China. E-mail: 409791715@qq.com; xiangfang8806@163.com; xkwang@xjtu.edu.cn; 1303118188@qq.com; wenchchen@xjtu.edu.cn (corresponding author).

²DataYes!, Shanghai 200080, China. E-mail: wei1.wang@datayes.com.

© 2022 Society of Exploration Geophysicists. All rights reserved.

system, and nonlinear effects within the vibrator itself, harmonic distortion exists in most land vibroseis recordings. The distortion can significantly obscure the correlated data, thus hindering subsequent seismic processing and stratigraphic interpretation. Researchers investigated the vibrator system mechanism and possible improvements to reduce the harmonic distortion in the output of ground forces (Wei et al., 2007, 2010).

However, limited by the metal nature of the baseplate, harmonic distortions are unavoidable in practice under various coupling conditions between the vibrator and ground, especially on hard and uneven ground. These harmonic interferences are then investigated in uncorrelated records and correlated data using signal processing methods (Baradello and Accaino, 2013). The pure deterministic phase-shift filter method developed by Li et al. (1995) was the first signal processing method to successfully eliminate harmonic distortions in the baseplate signal and correlation ghost sweeps. The use of filtering methods in practice has been widespread. Even so, the results are typically not optimal because it is intended for analyzing the uncorrelated data acquired by the traditional single-shot survey and may not be suitable for efficient slip-sweep acquisition methods. Using a harmonic prediction operator, Meunier and Bianchi (2002, 2005) estimate each harmonic and then recursively decompose uncorrelated data into the fundamental and harmonic components. By subtracting the harmonic noise from the original data, the suppression results usually have higher fidelity. By applying the anticorrelation operator, Zhang et al. (2012) separate the fundamental and harmonic components of the ground force signal and reduce harmonic distortions, which is highly applicable. Karsli and Dondurur (2018) develop an iterative trimmed and truncated mean filter approach for harmonic noise elimination. As a significant benefit, an exact estimation of the fundamental frequency of the harmonic noise is not required. Because the reduction of harmonic noise in uncorrelated seismic data is low efficiency and requires large amounts of storage, other methods are also proposed to eliminate the harmonic noise in correlated data. For example, Dal Moro et al. (2007) remove harmonic distortions using a technique based on a genetic algorithm. Sicking et al. (2009) predict and subtract the harmonic noise based on the recorded ground force. In addition to being very robust and efficient, this method does not require uncorrelated traces. In addition, a harmonic noise prediction operator was proposed without ground force signals (Wang et al., 2012). Abd El-Aal (2010, 2011) presents a strategy for upper harmonic noise attenuation in the correlated data by simulating harmonic distortions. This algorithm may suffer from a performance problem due to the absence of adaptation and the method used to estimate the amplitudes of the frequency domain after the Fourier transpose in intentionally small sliding windows. Most recently, Denisov et al. (2021) propose optimal recursive filtering to isolate harmonic noise from valuable signals.

In the past few decades, various signal processing techniques based on harmonic analysis have been developed, such as the wavelet transform, the shearlet transform, the ridgelet transform, and the curvelet transform. Their primary objectives are to depict the signal of interest sparsely or identify the specific characteristics. The basis functions used in these transformations can be thought of as waveform atoms, each with its own set of mathematical features and abilities to define the characteristics of the signals that are being transformed. Generally speaking, if the signal can be constructed by the linear combination of a minimal number of basis atoms, then

that means the transform offers a sparse representation of the signal. The sparse representation is also widely used in seismic signal processing. Yarham and Herrmann (2008) remove the ground roll by curvelet-domain sparsity. As described by Bößmann and Ma (2015), seismic absorption decay signals are sparsely represented using a Gaussian chirplet model. Xu et al. (2016) develop a seismic model based on sparse representation and divide the seismic recording into the reflection and ground roll parts. As shown by their successful performance in the synthetic seismic data example and the application to seismic field data, the strong-energy ground roll is significantly reduced. Moreover, by using the sparse representation model, the reflected wave waveform is successfully preserved. Similarly, harmonic noise reduction also uses this technique. Yu and Garossino (2005) propose frequency-dependent noise attenuation (FDNAT), which decomposes the seismic signal with wavelet transform. Wang et al. (2018) train an adaptive dictionary and suppress the harmonic distortions based on the diverse waveform morphologies between the useful signals and harmonic noise.

Sparse representation has made significant achievements in recent years. Only one specific transform is usually highly ineffective when representing complicated field seismic signals. The ideas naturally turn out to form an overcomplete dictionary by incorporating several distinctive transforms, potentially showing the promising capability to represent complex seismic signals sparsely. As a typical case of constructing an overcomplete dictionary, morphological component analysis (MCA) was introduced and achieved good results. For example, Turquais et al. (2016) propose a sparsity promoting morphological decomposition to suppress coherent noise. In addition, MCA also can be applied to robust dip estimation (Cai and Ma, 2019) and acquisition footprint suppression (Liu et al., 2021).

The commonly used methods either depend on sweep and ground force signals or suffer from the complexity of harmonic noise. This paper proposes a technique using redundant waveform dictionaries to model and distinguish different signal components by considering their time-frequency spectra diversity. Following the assumption of MCA, two various waveform dictionaries are selected to characterize useful signals and harmonic noise, respectively. The separation is facilitated by iteratively exploring the sparsity of one signal component in the overcomplete dictionary while keeping the other component fixed. Results from synthetic and field data show the effectiveness of the proposed method.

METHODS

Starck et al. (2004) develop the MCA theory, which decomposes the signal into several components sparsely using the overcomplete dictionary. The MCA makes the two following assumptions.

Assumption 1: The signal is assumed to be a linear superposition of n distinct morphological features, whereas each is sparsely represented by one corresponding separate dictionary. In other words, each signal component can be described with a dictionary Φ_k and the corresponding sparse representation \mathbf{x}_k . The signal can be expressed as follows:

$$\mathbf{s} = \sum_{k=1}^n \mathbf{s}_k = \sum_{k=1}^n \Phi_k \mathbf{x}_k. \quad (1)$$

Assumption 2: MCA assumes that, for every specific component s_k , one appropriate dictionary used for decomposition can produce a

highly sparse representation, whereas the other dictionaries $\Phi_{j \neq k}$ can only provide nonsparse decomposition, that is,

$$\forall \{k, j\} \in \{1, \dots, n\}; j \neq k \Rightarrow \|\Phi_k^T \mathbf{s}_k\|_0 < \|\Phi_j^T \mathbf{s}_k\|_0. \quad (2)$$

The l_0 norm measures sparseness, which means that the sparsest decomposition has the fewest nonzero coefficients.

With these two assumptions satisfied, we can provide the sparsity-promoted signal separation model. The following optimization model calculates the decomposition coefficients \mathbf{x}_k for representing the corresponding signal components:

$$\arg \min_{\{\mathbf{x}_1, \dots, \mathbf{x}_n\}} \sum_{k=1}^n \|\mathbf{x}_k\|_0 \quad \text{subject to } \mathbf{s} = \sum_{k=1}^n \Phi_k \mathbf{x}_k. \quad (3)$$

The optimization problem consists of two terms. One is the objective function by minimizing the sparseness measure, and the other is the data-fit term. However, this problem is a nondeterministic polynomial (NP)-hard problem because of the use of the l_0 norm. The MCA method makes this optimization problem solvable by substituting the l_0 norm by l_1 norm and relaxing the equality constraint through minimizing (Starck et al., 2005)

$$\arg \min_{\{\mathbf{s}_1, \dots, \mathbf{s}_n\}} \lambda \sum_{k=1}^n \|\Phi_k^T \mathbf{s}_k\|_1 + \frac{1}{2} \|\mathbf{s} - \sum_{k=1}^n \mathbf{s}_k\|_2^2. \quad (4)$$

According to morphologic appearance in slip-sweep correlated recordings, seismic data primarily comprise body waves, ground roll, harmonic distortion, and random noise (Li et al., 2015). Here, we discuss the attenuation of harmonic noise. Meanwhile, the body and ground roll waves are referred to as the signal components (abbreviated as the signal), whereas harmonic noise is the noise component. A seismic record is then expressed as

$$\mathbf{s} = \mathbf{s}_r + \mathbf{s}_h + \mathbf{s}_n, \quad (5)$$

where \mathbf{s}_r represents the signal, \mathbf{s}_h represents the harmonic noise, and \mathbf{s}_n is the random noise. Separating the signal from harmonic noise with MCA seeks to solve

$$\arg \min_{\{\mathbf{x}_r, \mathbf{x}_h\}} \|\mathbf{x}_r\|_1 + \|\mathbf{x}_h\|_1, \quad \text{s.t. } \|\mathbf{s} - \Phi_r \mathbf{x}_r - \Phi_h \mathbf{x}_h\|_2^2 \leq \epsilon, \quad (6)$$

where Φ_r and Φ_h , playing a role of discriminants between the signal \mathbf{s}_r and harmonic noise \mathbf{s}_h , are the sparse representation dictionary for signal \mathbf{s}_r and harmonic noise \mathbf{s}_h , respectively. The vectors of signal and harmonic noise coefficient are \mathbf{x}_r and \mathbf{x}_h , respectively, and ϵ is a threshold for reconstruction error and represents an estimate of random noise. An unconstrained optimization problem can precisely replace the constrained optimization in equation 6 through an appropriate Lagrange multiplier:

$$\begin{aligned} \{\mathbf{x}_r^{\text{opt}}, \mathbf{x}_h^{\text{opt}}\} = \arg \min_{\{\mathbf{x}_r, \mathbf{x}_h\}} & \frac{1}{2} \|\mathbf{s} - \Phi_r \mathbf{x}_r - \Phi_h \mathbf{x}_h\|_2^2 \\ & + \lambda (\|\mathbf{x}_r\|_1 + \|\mathbf{x}_h\|_1). \end{aligned} \quad (7)$$

The minimization of the objective function in equation 7 can be handled by the block-coordinate relaxation (BCR) technique

through the iterative hard threshold operator to calculate optimized $\mathbf{x}_r^{\text{opt}}$ and $\mathbf{x}_h^{\text{opt}}$ (Bruce et al., 1998; Elad et al., 2005).

The MCA theory shows that the feasibility of separating signals relies on the inconsistency between dictionaries, and each dictionary should lead to sparse representations of the corresponding signal component. Thus, choosing proper signal representations is the critical issue for our problem.

The signal and harmonic noise have different time-frequency distribution characteristics, as shown in Figure 1. In general, useful seismic signals are represented as the convolution of the source wavelet and the reflectivity series. Therefore, useful signals after the wavelet transform produce localized regions centered on the dominant frequency of the source wavelet. In contrast, harmonic noise consists of slanted lines of varying slopes. Correspondingly, we can select two dictionaries with different time-frequency distributions to separate them. The wavelet transform is one efficient tool for sparsely representing seismic signals because the mother wavelet function is similar to the seismic wavelet. Therefore, we anticipate that useful signals, such as body waves and ground roll, are prone to be sparsely represented with the wavelet transform. However, harmonic noise is well known for its linear distribution in the time-frequency domain. Technically speaking, a tailored tool, namely, the chirplet transform, is ideally suited for analyzing chirp-like signals. Its time-frequency atoms are best suited to describe such kinds of signal components. Thus, we use the chirplet transform as the representative dictionary for harmonic noise components.

Wavelet transform

Wavelet analysis is used to convert the investigated signal into a desirable temporal and spectral representation, contributing to signal analysis and processing improvement. Usually, the mother wavelet should have the same waveform as the reflected wavelet. The continuous wavelet transform of the signal $s(t)$ is defined as the correlation between the signal and the dilated and shifted wavelets as follows:

$$\text{WT}_s(a, \tau) = \frac{1}{\sqrt{a}} \int_{-\infty}^{\infty} s(t) \psi^* \left(\frac{t - \tau}{a} \right) dt, \quad (8)$$

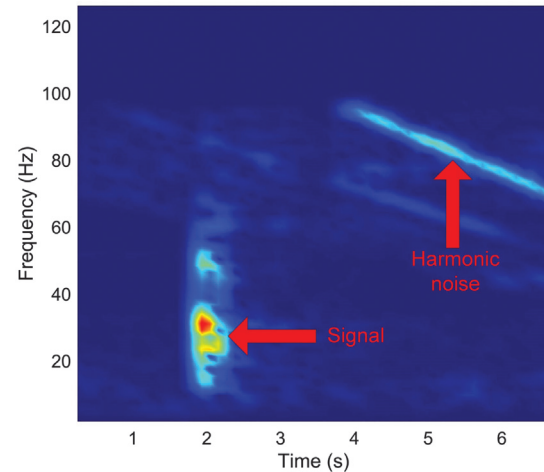


Figure 1. The time-frequency distribution of a typical seismic trace contaminated by harmonic noise.

where a is the scaling factor; τ denotes the time shift; $\psi(t)$ corresponds to the mother wavelet, such as shown in Figure 2a; the asterisk represents the complex conjugate operation. After MCA separation, the denoised data can be calculated by

$$\hat{s}_r(t) = \frac{1}{C^\psi} \int_\tau \int_a \frac{1}{a^2} \text{WT}_s(a, \tau) \psi\left(\frac{t-\tau}{a}\right) da d\tau, \quad (9)$$

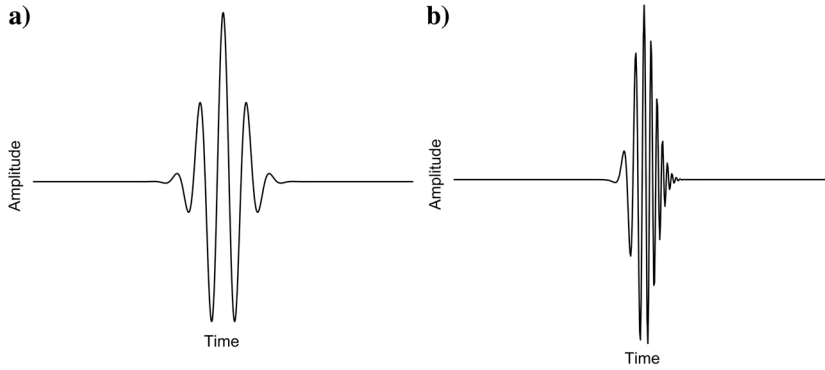


Figure 2. (a) Continuous wavelet transform's kernel function and (b) chirplet transform's kernel function modulated by a Gaussian function.

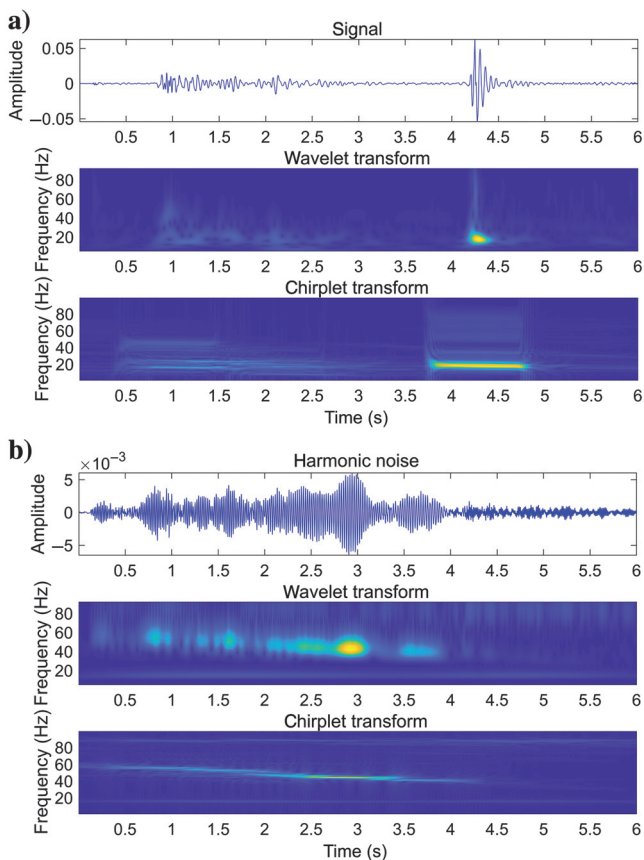


Figure 3. The sparsity comparison with wavelet transform and chirplet transform. (a) The sparsity of signal obtained by wavelet transform and chirplet transform and (b) the sparsity of harmonic noise obtained by wavelet transform and chirplet transform.

where the admissibility condition is satisfied by $C^\psi = \int_R ((|\Psi(\omega)|^2)/\omega) d\omega < +\infty$, and $\Psi(\omega)$ is the Fourier transform of $\psi(t)$.

Chirplet transform

As a time-frequency representation technique, the chirplet transform (Mann and Haykin, 1995) uniquely incorporates a frequency-dependent resolution with the simultaneous localization of the real and imaginary spectra. By manipulating the basis function with the shift, shear, and scaling operators, a 5D parameter space for the energy density is obtained. By time and frequency shift, as well as by time shift and scaling, this space includes projections of the appropriate densities obtained from a short-time Fourier transform, as well as projections of a wavelet transform. It is worth noting that the chirp operation on the frequency axis is omitted to fit the waveform of the harmonic noise better, resulting in a more accurate representation of the harmonic noise. In mathematical form, the chirplet transform can be formulated as follows:

$$\text{CT}_s(t, f, a, c) = \int s(\tau) h^*(\tau - t, f, a, c) d\tau, \quad (10)$$

where

$$h(t, f, a, c) = g\left(\frac{t}{a}\right) e^{j\pi 2ft + j\pi c\left(\frac{t}{a}\right)^2} \quad (11)$$

and

$$g(t) = \left(\frac{1}{\sqrt{2\pi}\sigma} e^{-\frac{1}{2}\left(\frac{t}{\sigma}\right)^2} \right)^{\frac{1}{2}}. \quad (12)$$

Similarly, a denotes a scaling parameter, c corresponds to a linear frequency modulation factor, and $h(t, f, a, c)$ is the chirplet kernel function modulated by a Gaussian function $g(t)$ (Figure 2b). After the MCA separation, the suppressed harmonic noise can be computed by

$$\hat{s}_h(t) = \int_c \int_a \int_f \int_\tau \text{CT}_s(t, f, a, c) h(\tau - t, f, a, c) d\tau df da dc, \quad (13)$$

which is the inverse chirplet transform.

Sparsity analysis

Figure 3 illustrates the time-frequency analysis of the signal and the separated harmonic distortion by the proposed method. Wavelet and chirplet transforms are applied to decompose the signal and isolate harmonic noise. The comparison is obvious and intuitive. The wavelet transform is prone to capturing the transient variations of signals but spreads its delineation for the linear structures in the time-frequency domain. In contrast, the chirplet transform is better

fitted to characterize the linear time-frequency relationship but fails to render the characteristics of transient signals. The sparsity of each signal component is measured in the two transform domains and listed in Table 1. The sparsity comparison again proves our observations. The signal is represented by much fewer nonzero coefficients in the wavelet domain, whereas the harmonic noise shows much fewer nonzero coefficients in the chirplet domain. Therefore, the two dictionaries that we choose are suitable and satisfy the MCA assumptions.

EXAMPLES

This section illustrates applications of the proposed method by suppressing the harmonic noise of synthetic data and a field seismic data set.

Synthetic data test

To verify our method's effectiveness of harmonic noise suppression, we first evaluate our approach on synthetic model data, as displayed in Figure 4a. This model comprises 301 traces and has a temporal resolution of 0.002 s. In Figure 4a, it is noticeable that harmonic noise marked by the arrow severely contaminates

Table 1. The sparsity comparison of different signal components using wavelet transform and chirplet transform.

Dictionaries	Signal	Harmonic noise
Wavelet transform	0.0337	0.1709
Chirplet transform	0.1821	0.0155

The sparsity is measured by the ratio between the number of nonzero coefficients and the dimension of the coefficient vector.

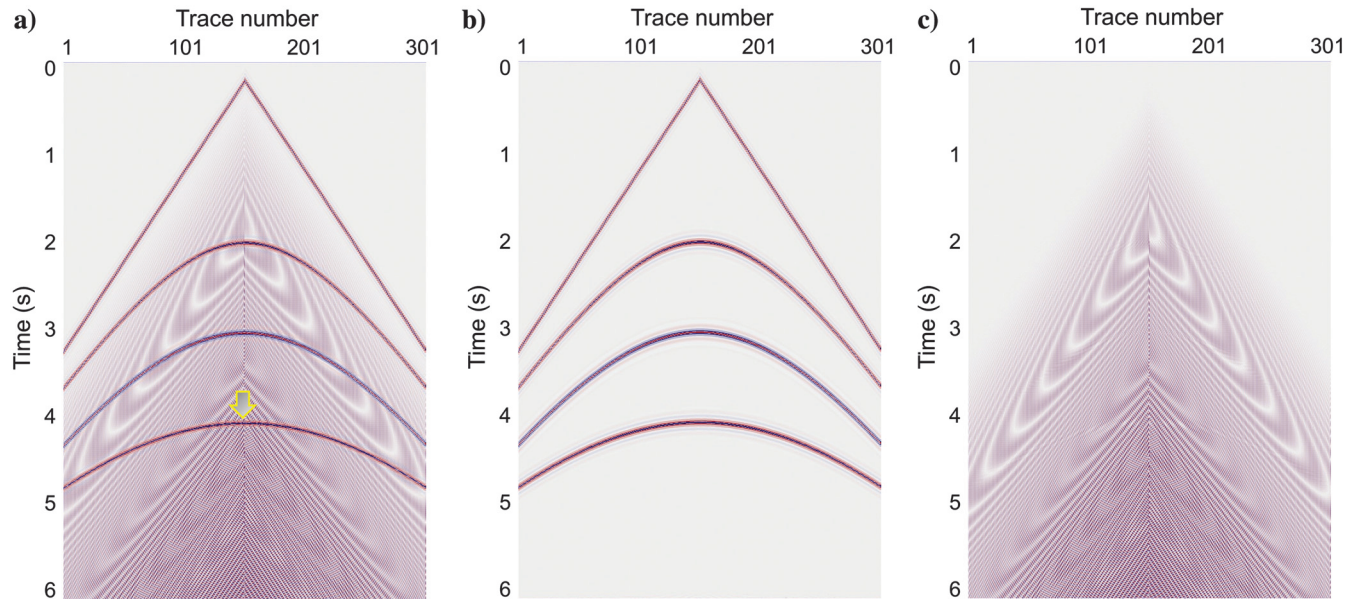


Figure 4. The results of signal and harmonic noise separation by our proposed method: (a) the original records, (b) the obtained signal, and (c) the removed harmonic noise. Our proposed method successfully suppresses harmonic noise with minimal degradation of useful signals, despite the fact that the harmonic noise marked by the arrow in (a) severely contaminates useful signals.

the original data, posing significant problems to interpretation. Figure 4b and 4c illustrates the signal and noise separation results, respectively, obtained by the proposed method. From an in-depth comparison of Figure 4b with Figure 4a, we can see the success of harmonic noise reduction. The results of the 100th trace in Figure 4 are shown in Figures 5 and 6. Comparing the original signal with the separated signals and separated harmonic distortion in the spatial-temporal domain in Figure 5, high-fidelity signals are successfully recovered, and harmonic distortion is eliminated effectively. Figure 5 shows that our approach offers the primary benefit of preserving the signal with high fidelity. Likewise, from the results in the time-frequency domain, we can observe that the distributions of the valuable signal exhibit different characteristics from

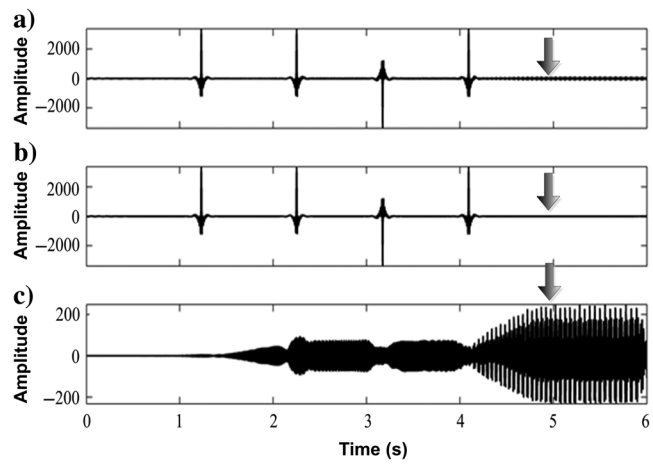


Figure 5. The analysis of the 100th trace data extracted from Figure 4 in the time domain: (a) the original records, (b) the recovered signal, and (c) the removed harmonic distortion.

the removed harmonic noise which corresponds to oblique lines, thus confirming the successful elimination of harmonic noise.

Field seismic data test

The results from the synthetic data indicate that the proposed approach can remove harmonic noise effectively with satisfactory preservation of the high-fidelity signal. To further illustrate the

effectiveness of the proposed method for harmonic noise attenuation, we apply it to a section of a correlated slip-sweep seismic record acquired from western China, as shown in Figure 7a. This seismic field data set includes 396 traces with a trace interval of 25 m, and the temporal interval is 0.002 s. Using the proposed method to separate signals and harmonic noise, we set the iteration number of MCA to 30, and λ decreases exponentially from 800 to the average Fourier transform value of each trace data. The parameters

Figure 6. The analysis of the 100th trace data extracted in Figure 4 in the time-frequency domain: (a) the original records, (b) the recovered signal, and (c) the removed harmonic distortion.

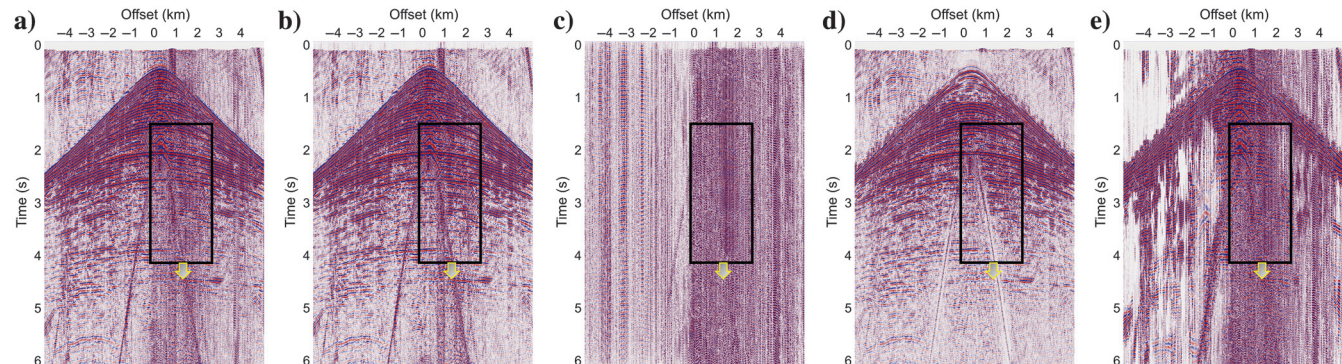
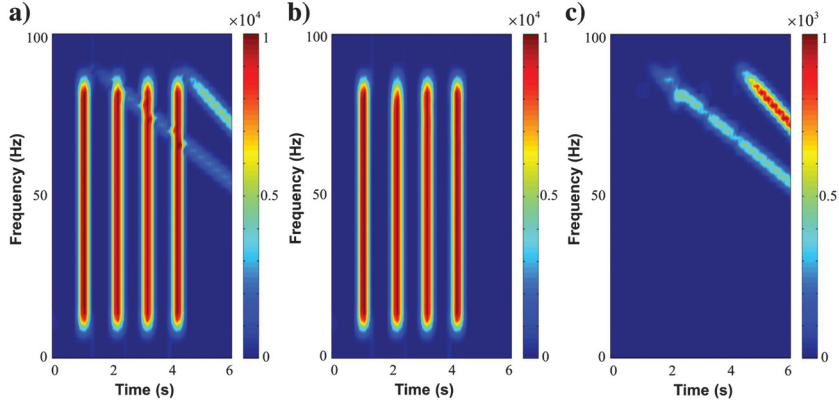


Figure 7. Field data results. (a) Original seismic record, (b) recovered signals by our proposed method, (c) removed harmonic noise by our proposed method, (d) recovered signals by FDNAT, and (e) removed harmonic noise by FDNAT. The arrows indicate that FDNAT causes signal leakage, but the proposed method preserves the structure of the signal better. The black boxes depict the magnified area for Figure 8.

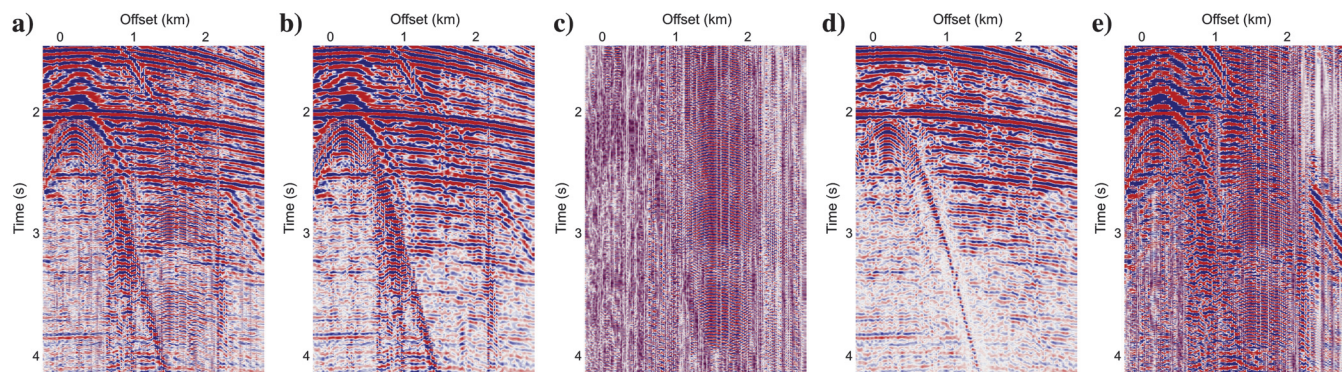


Figure 8. (a-e) Magnified view of the results bounded by the black box in Figure 7a-7e, respectively. (a) Original seismic record, (b) recovered signals by our proposed method, (c) removed harmonic noise by our proposed method, (d) recovered signals by FDNAT, and (e) removed harmonic noise by FDNAT.

a and *c* of the chirplet transform are kept at a constant value of 0.5 and 1.0, respectively. The Gaussian function length is set to be 512. The continuous wavelet transform has 54 decomposition scales.

The FDNAT method (Yu and Garossino, 2005), which attenuates harmonic noise in decomposed frequency bands after being transformed into the time-frequency domain by a time-frequency analysis tool, is commonly used in industry. By using frequency-dependent and time-variant amplitude threshold values in defined trace neighborhoods, it can detect and suppress noise corresponding to different frequency ranges and time windows. The threshold values can be calculated adaptively by calculating the average amplitude of sampling points in the time window. The strong adaptability and easy implementation make FDNAT a widely used module to suppress harmonic noise in commercial software applications, so we choose it as our baseline method. To apply FDNAT, we set the trace window size as 21, the time window size as 400 ms (200 samples), the sliding time window as 200 ms (100 samples), and every 10 Hz between 3 and 83 Hz makes up the decomposed frequency bands.

The elimination results of harmonic noise are displayed in Figure 7b–7e. Comparing the signals obtained by the proposed approach in Figure 7b with the signals obtained by the FDNAT method in Figure 7d, the FDNAT method seems to suppress more noise and output a better noise-free result. However, the proposed method preserves signal better, especially for typical first breaks and shallow reflections. Comparing the harmonic noise obtained by our approach in Figure 7c with the harmonic noise removed by the FDNAT method in Figure 7e, we also verify the effectiveness of the proposed method from the separated harmonic noise aspect. Our approach can precisely identify and extract the harmonic noise with little signal energy observed in the estimated noise panel. However, there is noticeable signal leakage in the noise estimation of the FDNAT method. We can see the superior performance of the proposed method in Figure 8 with the magnified rectangle areas marked in Figure 7.

The 256th trace located at 1.45 km of the original record and the corresponding signal parts generated by the proposed method and the FDNAT method are shown in Figure 9. Furthermore, their corresponding spectra are analyzed in Figure 10. Compared with the proposed method, the FDNAT method damages useful signals, primarily the late reflections. The result obtained by the proposed method is more reliable and has less signal leakage. We also can prove it from their spectra because the high-frequency energy of our approach is smaller. Then, we stack the original prestack data in Figure 11a. The stacked section shows apparent harmonic noise disturbances. Denoising harmonic noise with these two methods results in significantly improved stacked profiles, as shown in Figure 11b and 11d. However, the result obtained by the proposed method shows a higher signal-to-noise ratio and more coherent reflections and is also favorable for thin-bed reflections. The spectra

of three stacked data for comparison are shown in Figure 12. We can see that the spectra of the proposed method and FDNAT are very similar, but the energy of our method is slightly higher than that of FDNAT. The higher energy is because the fidelity of our method is better than FDNAT, which means that the waveform consistency of our useful signals is better than FDNAT. Hence, the stacked signals

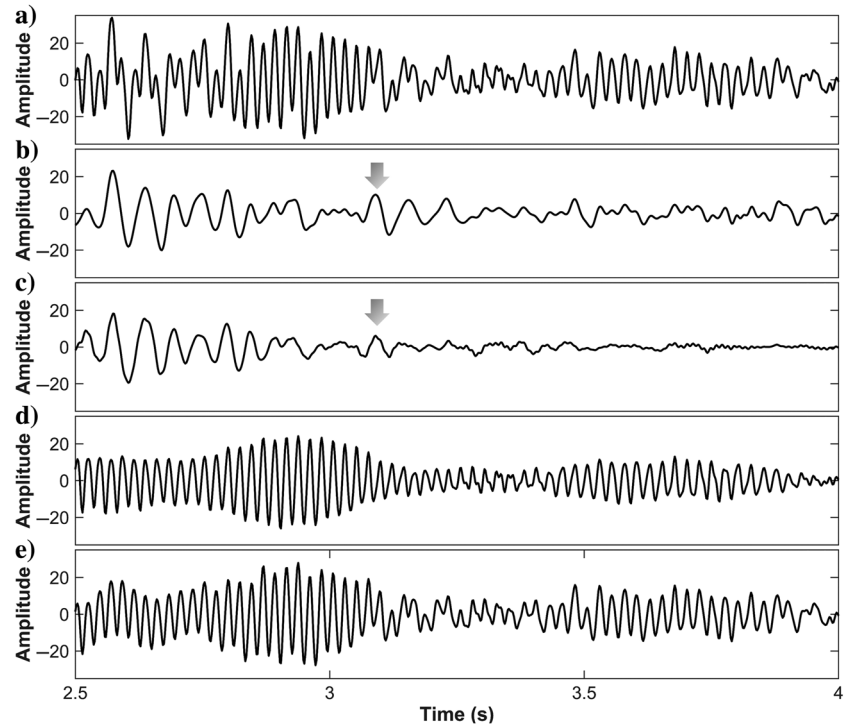


Figure 9. Comparison of the separation results with the 256th trace data which is located at 1.45 km in Figure 7. (a) The original records, (b) the recovered signal by the proposed method, (c) the recovered signal by FDNAT, (d) removed noise by the proposed method, and (e) removed noise by FDNAT. It can be seen that, in comparison to the proposed method, the FDNAT method causes obvious damage to the deep-layer effective wave, as indicated by the arrows in (b and c). Furthermore, after the reduction of harmonic noise using the FDNAT method, residual harmonic energy can be detected in the deep layer.

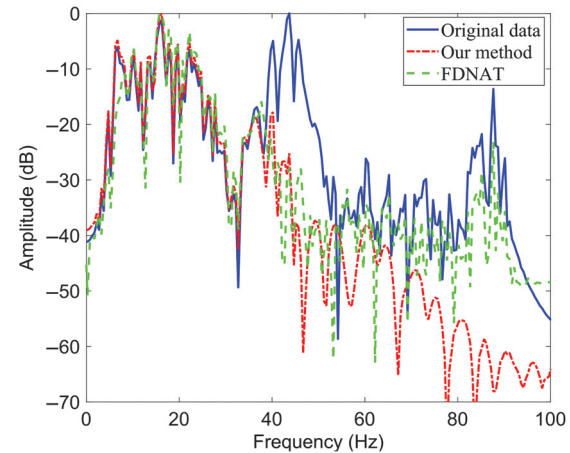


Figure 10. The corresponding spectra of the data shown in Figure 9 for a time window of 1.5–4.0 s.

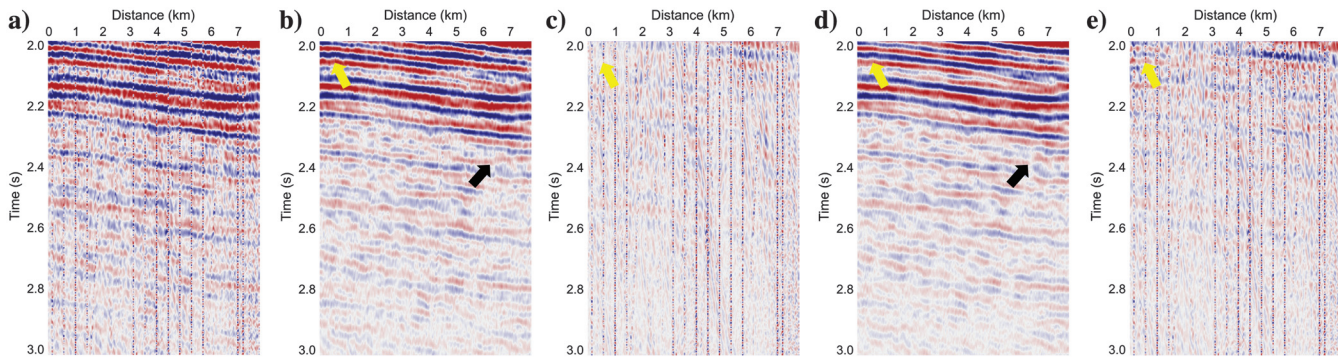


Figure 11. Stacked profiles. (a) Original seismic record, (b) recovered signals by the proposed method, (c) noise removed by the proposed method, (d) recovered signals by FDNAT, and (e) noise removed by FDNAT. Black arrows indicate that the result obtained by the proposed method has a higher signal-to-noise ratio and more coherent reflections. When examining the regions indicated by yellow arrows, it is evident that FDNAT damages the useful signals, whereas our proposed method has a higher fidelity.

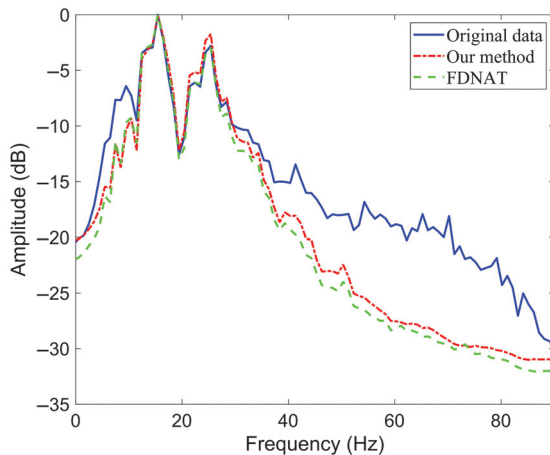


Figure 12. The spectra of the stacked data shown in Figure 11.

have a higher amplitude. These results also prove the effectiveness of our proposed method.

CONCLUSION

In this work, we propose a practical approach to suppress harmonic noise in slip-sweep data. Our method is based on MCA and exploits waveform differences between useful reflections and harmonic interferences. The construction of the different waveform dictionaries, also known as mathematical transformations, is an essential step. To sparsely represent the signal and harmonic noise, the wavelet transform and chirplet transform are used, respectively. The signal and harmonic noise are then iteratively separated using the BCR method. The results of the synthetic data and field slip-sweep data show that our method successfully eliminates the harmonic noise while causing no noticeable damage to useful signals. Furthermore, our approach is not dependent on the ground force signal. As a result, processing effectiveness may be substantially increased compared with techniques that rely on ground force signals. The presented method is data-driven and implemented trace-by-trace. Therefore, it is more convenient and robust than the schemes of suppressing harmonic noise from the shot data. In addition,

single-trace processing makes it easy for parallel computing to meet practical requirements.

ACKNOWLEDGMENTS

This research is sponsored by the National Natural Science Foundation of China (41774135 and 41974131). Many thanks go to the assistant editor A. Guittot, the associate editor Y. Zhao, and other anonymous reviewers for their insightful suggestions. We are grateful to L. Jiang and X. Yang from Xinjiang Oilfield Company for assistance in performing FDNAT on field seismic data.

DATA AND MATERIALS AVAILABILITY

Data associated with this research are available and can be obtained by contacting the corresponding author.

REFERENCES

- Abd El-Aal, A. K., 2010, Eliminating upper harmonic noise in vibroseis data via numerical simulation: *Geophysical Journal International*, **181**, 1499–1509, doi: [10.1111/j.1365-246X.2010.04594.x](https://doi.org/10.1111/j.1365-246X.2010.04594.x).
- Abd El-Aal, A. K., 2011, Harmonic by harmonic removal technique for improving vibroseis data quality: *Geophysical Prospecting*, **59**, 279–294, doi: [10.1111/j.1365-2478.2010.00918.x](https://doi.org/10.1111/j.1365-2478.2010.00918.x).
- Baradello, L., and F. Accaino, 2013, Vibroseis deconvolution: A comparison of pre and post correlation vibroseis deconvolution data in real noisy data: *Journal of Applied Geophysics*, **92**, 50–56, doi: [10.1016/j.jappgeo.2013.02.009](https://doi.org/10.1016/j.jappgeo.2013.02.009).
- Bößmann, F., and J. Ma, 2015, Asymmetric chirplet transform for sparse representation of seismic data: *Geophysics*, **80**, no. 6, WD89–WD100, doi: [10.1190/geo2015-0063.1](https://doi.org/10.1190/geo2015-0063.1).
- Bruce, A. G., S. Sardy, and P. Tseng, 1998, Block coordinate relaxation methods for nonparametric signal denoising: *Aerospace/Defense Sensing and Controls, International Society for Optics and Photonics*, 75–86.
- Cai, K., and J. Ma, 2019, Robust estimation of multiple local dips via multi-directional component analysis: *IEEE Transactions on Geoscience and Remote Sensing*, **57**, 2798–2810, doi: [10.1109/TGRS.2018.2877702](https://doi.org/10.1109/TGRS.2018.2877702).
- Dal Moro, G., P. Scholtz, and K. Iranpour, 2007, Harmonic noise attenuation for vibroseis data: 27th National Group for Solid Earth Geophysics 3, 511–513.
- Denisov, M. S., A. A. Egorov, and M. B. Shneerson, 2021, Optimization-based recursive filtering for separation of signal from harmonics in vibroseis: *Geophysical Prospecting*, **69**, 779–798, doi: [10.1111/1365-2478.13084](https://doi.org/10.1111/1365-2478.13084).
- Elad, M., J. L. Starck, P. Querre, and D. L. Donoho, 2005, Simultaneous cartoon and texture image inpainting using morphological component analysis (MCA): *Applied & Computational Harmonic Analysis*, **19**, 340–358, doi: [10.1016/j.acha.2005.03.005](https://doi.org/10.1016/j.acha.2005.03.005).

- Karsli, H., and D. Dondurur, 2018, A mean-based filter to remove power line harmonic noise from seismic reflection data: *Journal of Applied Geophysics*, **153**, 90–99, doi: [10.1016/j.jappgeo.2018.04.014](https://doi.org/10.1016/j.jappgeo.2018.04.014).
- Lebedev, A. V., and I. A. Beresnev, 2004, Nonlinear distortion of signals radiated by vibroseis sources: *Geophysics*, **69**, 968–977, doi: [10.1190/1.1778240](https://doi.org/10.1190/1.1778240).
- Li, X., W. Chen, W. Wang, X. Wang, and Y. Zhou, 2015, Harmonic noise removal in united time-frequency domain via sparse promotion: 85th Annual International Meeting, SEG, Expanded Abstracts, 4725–4729, doi: [10.1190/segam2015-5877902.1](https://doi.org/10.1190/segam2015-5877902.1).
- Li, X., W. Soellner, and P. Hubral, 1995, Elimination of harmonic distortion in vibroseis data: *Geophysics*, **60**, 503–516, doi: [10.1190/1.1443787](https://doi.org/10.1190/1.1443787).
- Liu, D., L. Gao, X. Wang, and W. Chen, 2021, A dictionary learning method with atom splitting for seismic footprint suppression: *Geophysics*, **86**, no. 6, V509–V523, doi: [10.1190/geo2020-0681.1](https://doi.org/10.1190/geo2020-0681.1).
- Mann, S., and S. Haykin, 1995, The chirplet transform: Physical considerations: *Transactions on Signal Processing*, **43**, 2745–2761, doi: [10.1109/78.482123](https://doi.org/10.1109/78.482123).
- Meunier, J., and T. Bianchi, 2002, Harmonic noise reduction opens the way for array size reduction in vibroseis operations: 72nd Annual International Meeting, SEG, Expanded Abstracts, 70–73, doi: [10.1190/1.1817354](https://doi.org/10.1190/1.1817354).
- Meunier, J., and T. Bianchi, 2005, Cost-effective, high density vibroseis acquisition: 75th Annual International Meeting, SEG, Expanded Abstracts, 44–47, doi: [10.1190/1.2142239](https://doi.org/10.1190/1.2142239).
- Sicking, C., T. Fleure, S. Nelan, and B. McLain, 2009, Slip sweep harmonic noise rejection on correlated shot data: 79th Annual International Meeting, SEG, Expanded Abstracts, 36–39, doi: [10.1190/1.3255636](https://doi.org/10.1190/1.3255636).
- Starck, J.-L., M. Elad, and D. Donoho, 2004, Redundant multiscale transforms and their application for morphological component separation: *Advances in Imaging and Electron Physics*, **132**, 287–348, doi: [10.1016/S1076-5670\(04\)32006-9](https://doi.org/10.1016/S1076-5670(04)32006-9).
- Starck, J.-L., Y. Moudden, J. Bobin, M. Elad, and D. Donoho, 2005, Morphological component analysis: *Proceedings of SPIE*, **5914**, 59140Q, doi: [10.1117/12.615237](https://doi.org/10.1117/12.615237).
- Turquais, P., E. Asgedom, and W. Söllner, 2016, Sparsity promoting morphological decomposition for coherent noise suppression: Application to streamer vibration related noise: 86th Annual International Meeting, SEG, Expanded Abstracts, 4639–4643, doi: [10.1190/segam2016-13856592.1](https://doi.org/10.1190/segam2016-13856592.1).
- Wang, B., H. Li, B. Zhao, Z. Huang, M. Zhang, and L. Mei, 2012, Cross-harmonic noise removal on slip-sweep vibroseis data: 82nd Annual International Meeting, SEG, Expanded Abstracts, 1–5, doi: [10.1190/segam2012-0059.1](https://doi.org/10.1190/segam2012-0059.1).
- Wang, H., X. Chen, Y. Zhou, J. Chen, and W. Chen, 2018, Harmonic noise suppression based on the classification of adaptive learning dictionary: International Geophysical Conference, 449–452.
- Wei, Z., T. F. Phillips, and M. A. Hall, 2010, Fundamental discussions on seismic vibrators: *Geophysics*, **75**, no. 6, W13–W25, doi: [10.1190/1.3509162](https://doi.org/10.1190/1.3509162).
- Wei, Z., J. J. Sallas, J. M. Crowell, and J. E. Teske, 2007, Harmonic distortion reduction on vibrators — Suppressing the supply pressure ripples: 77th Annual International Meeting, SEG, Expanded Abstracts, 51–55, doi: [10.1190/1.2792380](https://doi.org/10.1190/1.2792380).
- Xu, X., G. Qu, Y. Zhang, Y. Bi, and J. Wang, 2016, Ground-roll separation of seismic data based on morphological component analysis in two-dimensional domain: *Applied Geophysics*, **13**, 116–126, doi: [10.1007/s11770-016-0546-0](https://doi.org/10.1007/s11770-016-0546-0).
- Yarham, C., and F. J. Herrmann, 2008, Bayesian ground-roll separation by curvelet-domain sparsity promotion: 78th Annual International Meeting, SEG, Expanded Abstracts, 2576–2580, doi: [10.1190/1.3064092](https://doi.org/10.1190/1.3064092).
- Yu, Z., and P. G. Garossino, 2005, High-energy noise attenuation of seismic data in the wavelet-transform domain: *Integrated Computer-Aided Engineering*, **12**, 57–67, doi: [10.3233/ICA-2005-12105](https://doi.org/10.3233/ICA-2005-12105).
- Zhang, H.-J., H. Zhou, A. E. A. K. Abd El, and J. Zhang, 2012, The anti-correlation method for removing harmonic distortion in vibroseis slip-sweep data: *Applied Geophysics*, **9**, 159–167, doi: [10.1007/s11770-012-0325-5](https://doi.org/10.1007/s11770-012-0325-5).

Biographies and photographs of the authors are not available.